Predictive Value of Early Postoperative CT Imaging Parameters for Major Complications Following Thoracoscopic Segmentectomy

Ann. Ital. Chir., 2026 97, 6: 1104–1111
https://doi.org/10.62713/aic.4569

Wei Jiang[1], Meng Zhang[1], Dong Zhang[1]

[1]Department of Radiology, The First People's Hospital of Jiashan, 314100 Jiaxing, Zhejiang, China

AIM: This study aimed to systematically evaluate the independent predictive value and diagnostic performance of quantitative indices derived from early postoperative computed tomography (CT) imaging for predicting major complications (Clavien-Dindo grade ≥II) within 30 days after pulmonary segmentectomy.

METHODS: A total of 231 patients who underwent Video-Assisted Thoracoscopic Surgery (VATS) segmentectomy were retrospectively enrolled. On CT images obtained within 2–3 days postoperatively, the depth of pleural effusion, pneumothorax rate, lung re-expansion ratio, and maximum subcutaneous air thickness were measured. The primary outcome was the occurrence of Clavien-Dindo grade ≥II complications within 30 days. Univariate and multivariate logistic regression analyses were performed, and predictive performance was evaluated using the area under the curve (AUC).

RESULTS: Major complications occurred in 42 patients (18.2%). Multivariate analysis identified depth of pleural effusion (odds ratio [OR] = 1.213, 95% confidence interval [CI]: 1.107–1.329, $p < 0.001$), pneumothorax rate (OR = 1.201, 95% CI: 1.081–1.333, $p < 0.001$), lung re-expansion ratio (OR = 0.872, 95% CI: 0.809–0.940, $p < 0.001$), and maximum subcutaneous air thickness (OR = 1.438, 95% CI: 1.248–1.656, $p < 0.001$) as independent predictors. Receiver operating characteristic (ROC) analysis demonstrated that maximum subcutaneous air thickness had the highest predictive performance (AUC = 0.850), followed by pneumothorax rate (AUC = 0.831), lung re-expansion ratio (AUC = 0.785), and depth of pleural effusion (AUC = 0.783).

CONCLUSIONS: Quantitative indices derived from early postoperative CT scans may serve as reliable imaging biomarkers for predicting major complications after pulmonary segmentectomy, thereby facilitating early identification of high-risk patients and guiding individualized postoperative management.

Keywords: thoracoscopic segmentectomy; postoperative complications; CT imaging parameters; predictive value; risk factors

Introduction

Thoracoscopic segmentectomy has become a standard minimally invasive procedure for treating early-stage non-small cell lung cancer and select benign conditions, with its advantages in oncological efficacy and preservation of pulmonary function widely recognized [1–3]. However, as with all thoracic surgeries, postoperative complications such as prolonged air leak, pneumonia, respiratory failure, and arrhythmia remain significant factors adversely affecting patient recovery, prolonging hospital stay, and increasing healthcare costs [4,5]. Accurate identification of patients at high risk for postoperative complications is crucial for achieving individualized and precise postoperative management.

Current postoperative risk assessment primarily relies on clinical experience, preoperative physiological status, and intraoperative findings. Traditional imaging evaluation, such as chest radiography, largely relies on the subjective judgment of the attending physician, leading to significant inter-observer variability in assessing effusion volume, pneumothorax extent, and lung re-expansion, with inherent limitations in precise quantification [6,7]. Computed tomography (CT) provides non-overlapping cross-sectional images and is considered the gold standard for evaluating the postoperative thoracic cavity. However, in clinical practice, the interpretation of postoperative CT often remains at a qualitative or semi-quantitative descriptive level, failing to fully exploit its potential for quantitative information extraction [8].

In recent years, the rise of quantitative imaging and radiomics has opened new avenues for extracting reproducible, objective biomarkers from medical images [9, 10]. In thoracic surgery, preliminary studies have explored the association between CT-based quantitative indices and postoperative pulmonary complications [11,12]. Nevertheless, research specifically investigating the predictive value of early postoperative CT quantitative indices for major

Submitted: 28 January 2026 Revised: 22 April 2026 Accepted: 11 May 2026 Published: 10 June 2026
Correspondence to: Wei Jiang, Department of Radiology, The First People's Hospital of Jiashan, 314100 Jiaxing, Zhejiang, China (e-mail: jayweime2016@163.com).
Editor: Luca Bertolaccini

complications following segmentectomy—a procedure involving more complex anatomy and more precise parenchymal resection—remains insufficient. Therefore, this study aimed to systematically evaluate the independent predictive value and diagnostic performance of a series of objective quantitative indices extracted from early postoperative CT imaging obtained within 2–3 days after surgery. These indices include the depth of pleural effusion, pneumothorax rate, lung re-expansion ratio, and maximum subcutaneous air thickness for predicting major complications (Clavien-Dindo grade $\geq$II) within 30 days after thoracoscopic segmentectomy. The goal was to enable early, objective identification of high-risk patients, providing robust imaging evidence to support clinical intervention decisions.

Methods

Study Population

This observational, retrospective cohort study was designed to investigate the association between early postoperative CT quantitative indices and major complications after segmentectomy. The study protocol was approved by the Institutional Review Board of The First People's Hospital of Jiashan (2026 Research No. 009). The requirement for informed consent was waived, and the study adhered to the principles of the Declaration of Helsinki.

We systematically screened all patients who underwent surgery in the Department of Thoracic Surgery at The First People's Hospital of Jiashan between January 2023 and October 2025. Inclusion criteria were: (1) age $\geq$18 years; (2) scheduled, unilateral thoracoscopic segmentectomy for clinical stage I non-small cell lung cancer or pulmonary nodules suspicious for malignancy; (3) systematic or lobe-specific lymph node dissection; and (4) availability of standard-dose non-contrast chest CT scan data completed within 2–3 days postoperatively. Exclusion criteria included: (1) history of prior ipsilateral thoracic surgery; (2) preoperative neoadjuvant chemotherapy or radiotherapy; (3) severe preoperative comorbidities, including cardiac dysfunction (New York Heart Association (NYHA) class III–IV), pulmonary dysfunction (Forced Expiratory Volume in one second [FEV_1] $<$50% predicted), hepatic dysfunction (Child-Pugh class B–C), or renal dysfunction (creatinine $>$2.0 mg/dL); (4) major intraoperative complications (e.g., massive bleeding $>$1000 mL, emergency conversion due to hemodynamic instability, intraoperative cardiac events); and (5) CT scans unsuitable for quantitative analysis due to technical reasons (e.g., severe metal artifacts) or missing images. Patients with tumor size $>$2 cm were predominantly those with ground-glass-opacity-dominant lesions (consolidation-to-tumor ratio $<$0.5). Ultimately, a total of 231 patients were included in the study cohort.

Surgical Procedure and Perioperative Management

All surgeries were performed by three experienced senior thoracic surgeons using standard multiport or uniportal Video-Assisted Thoracoscopic Surgery (VATS) techniques. The surgical strategy (extent of segmental resection) was determined based on tumor location, segmental anatomy, and preoperative three-dimensional reconstruction planning. A single chest tube was routinely placed postoperatively and connected to a water-seal drainage system. The criteria for chest tube removal were: a drainage volume of $<$300 mL over 24 hours, absence of air leak, and satisfactory lung expansion on chest radiograph. All patients were managed according to our institution's enhanced recovery after surgery pathway.

Data Collection

The primary outcome measure was the occurrence of major complications within 30 days postoperatively, with severity defined and graded according to the Clavien-Dindo classification system. This study defined "major complications" as grade $\geq$II (complications requiring pharmacological or interventional treatment). These complications specifically included, but were not limited to: prolonged air leak ($>$5 days), pneumonia requiring intravenous antibiotics, respiratory failure requiring non-invasive or invasive ventilation, postoperative hemorrhage requiring transfusion or reoperation, symptomatic atrial fibrillation, and significant pleural effusion/empyema requiring puncture or drainage. Complication data were collected and verified through a systematic review of electronic medical records by two independent researchers, with discrepancies resolved by a third-party adjudicator.

Image acquisition: All CT scans were performed using the same 256-slice multidetector CT scanner (GE Revolution Apex 256, GE Healthcare, Chicago, IL, USA). Scanning parameters were standardized as follows: tube voltage 120 kV, automatic tube current modulation, slice thickness 0.625–1.25 mm, matrix 512 $\times$ 512. Patients were scanned in the supine position during breath-hold at end-expiration. All quantitative measurements were performed on a dedicated imaging processing workstation using the open-source software 3D Slicer (version 5.0.3, Brigham and Women's Hospital, Inc., Boston, MA, USA), following this procedure: Pleural Effusion Depth: On axial images, the vertical distance from the inner chest wall to the lung parenchyma or the opposite boundary of the effusion was measured at the widest point of the posterior pleural effusion (unit: mm). The mean value of bilateral measurements was used for analysis, whereas measurements from the operative side alone were used for unilateral surgery. Pneumothorax Rate: A semi-automatic volume rendering segmentation technique was employed. First, the ipsilateral hemithorax contour, expanding from apex to diaphragm, was manually outlined, after which the software automatically calculated the total hemithoracic volume

(V_hemithorax). Then, the gas region within the hemithorax was segmented by setting a threshold (–1000 to –200 HU), and the pneumothorax volume (V_pneumothorax) was calculated. Pneumothorax rate = (V_pneumothorax / V_hemithorax) × 100%. Lung Re-expansion Ratio: This index assesses the degree of postoperative lung expansion. A similar method was used to segment the postoperative lung parenchyma volume on the operative side (V_postop_lung). The mirrored volume of the contralateral healthy lung (V_contralateral_lung) or the predicted ipsilateral lung volume (V_predicted) based on patient height and sex using standard formulas served as the reference baseline. This study employed the contralateral lung volume method: Lung re-expansion ratio = (V_postop_lung / V_contralateral_lung) × 100%. Maximum Subcutaneous Air Thickness: On soft tissue windows (window width 400 HU, window level 40 HU), at the level where subcutaneous emphysema was most prominent in the neck or chest wall, the maximum anterior-posterior or left-right diameter of the air collection was measured (unit: mm). Complication data were collected and verified through a systematic review of electronic medical records by two independent researchers, using a predefined structured reporting template based on the Clavien-Dindo system to ensure uniform documentation and assessment criteria.

To ensure consistency and reliability of measurements, all assessments were performed independently by two trained observers who were blinded to clinical outcomes and complications. The images were anonymized and de-identified prior to review, and the examinations were analyzed in a randomized sequence. The mean values of the two observers' measurements were used for final analysis. Complication data were collected and verified through a systematic review of electronic medical records by two independent researchers, using a predefined structured reporting template based on the Clavien-Dindo system to ensure uniform documentation and assessment criteria.

Statistical Analysis

The Shapiro–Wilk test was used to assess the normality of continuous variables. Continuous variables were expressed as mean ± standard deviation or median (interquartile range) based on their distribution. Comparisons between groups were performed using an independent samples *t*-test or Mann-Whitney U test. Categorical variables were expressed as frequency (percentage), and comparisons between groups were performed using the chi-square test or Fisher's exact test.

To identify predictors of major complications, between-group comparisons were first performed for all candidate variables. Only variables with $p < 0.05$ in these comparisons were entered into the multivariate stepwise regression analysis. Stepwise regression was used to construct the final prediction model. To evaluate the discriminatory ability of each independent CT predictor in the final model and the combined model, receiver operating characteristic (ROC) curves for predicting major complications were plotted, and the area under the curve (AUC) was calculated. As the lung re-expansion ratio was a protective factor (odds ratio <1) in the logistic regression model, its value was inversely transformed (i.e., 100 – ratio) for ROC analysis to ensure the consistent directional interpretation. To account for potential overfitting and model optimism, internal validation was performed using bootstrap resampling with 1000 iterations. Optimism-corrected AUC values were calculated for each predictor and the combined model. A p-value < 0.05 was considered statistically significant.

Results

Complication Rates After VATS Segmentectomy

A total of 231 patients who underwent VATS segmentectomy were included. Major postoperative complications occurred in 42 patients, yielding an incidence rate of 18.2%. The most common complication was prolonged air leak (15 cases, 35.7%), followed by pneumonia (11 cases, 26.2%) and atrial fibrillation (8 cases, 19.0%) (Table 1).

Comparison of Baseline Characteristics and CT Indices Between Groups

A comparison of baseline clinicopathological characteristics between the complication group and the no-complication group is presented in Table 2. No statistically significant differences were observed between the two groups regarding age, sex, body mass index (BMI), pulmonary function (Forced Expiratory Volume in one second [FEV_1] %, Diffusing Capacity of the Lungs for Carbon Monoxide [DLCO] %), comorbidities (hypertension, diabetes, coronary artery disease, Chronic Obstructive Pulmonary Disease [COPD]), smoking history, tumor characteristics (size and stage), or surgery-related variables (operation time, intraoperative blood loss) (all $p > 0.05$). Chest tube duration and postoperative hospital stay are now reported in Table 2 (both $p < 0.001$).

Early postoperative CT quantitative indices showed highly significant differences between the two groups. Compared with the no-complication group, the complication group had significantly greater depth of pleural effusion, pneumothorax rate, and maximum subcutaneous air thickness, while the lung re-expansion ratio was significantly lower (all $p < 0.001$).

Multivariate Analysis

The duration of chest tube drainage and the length of postoperative hospital stay were not included in the multivariate logistic regression model, as they were considered variables associated with postoperative outcomes rather than early predictors of major complications. Consequently, this multivariate model was restricted to including early postoperative quantitative CT parameters with potential predictive relevance. The results confirmed that all were independent

Table 1. Complication rates after VATS segmentectomy.

Complication type	Prolonged air leak	Pneumonia	Atrial fibrillation	Others
Cases, n (%)	15 (35.7%)	11 (26.2%)	8 (19.0%)	8 (19.0%)

VATS, Video-Assisted Thoracoscopic Surgery.

predictors of major postoperative complications (Table 3). Specifically, for each unit increase in pleural effusion depth and pneumothorax rate, the risk of complications increased by 21% and 20%, respectively. For each 1 mm increase in maximum subcutaneous air thickness, the risk increased by 44%. The lung re-expansion ratio was identified as a protective factor (OR = 0.872).

Evaluation of Predictive Performance of CT Quantitative Indices

To assess the discriminatory ability of the four CT quantitative indices, receiver operating characteristic curves for predicting major complications were plotted, and the area under the curve was calculated for each. The results indicated that all four indices demonstrated good predictive performance (Fig. 1). Maximum subcutaneous air thickness showed the highest discriminatory ability, with an AUC of 0.850 and an optimal cutoff value of 10.5 mm. Pneumothorax rate demonstrated an AUC of 0.831, with an optimal cutoff value of 8.5%. The AUCs for lung re-expansion ratio and pleural effusion depth were 0.785 and 0.783, respectively, with the optimal cutoff values of 80.5% and 16.5 mm. The combined model incorporating all four CT parameters yielded an apparent AUC of 0.961. After optimism correction using 1000 bootstrap resamples, the corrected AUC was 0.956 (optimism = 0.005), indicating excellent and robust discriminatory ability. The predictive performance of each CT parameter and the combined model is summarized in Table 4.

Discussion

This study systematically evaluated the predictive value of four quantitative indices derived from early postoperative (within 2–3 days) CT imaging for major complications following thoracoscopic segmentectomy. The main findings of this study were that depth of pleural effusion, pneumothorax rate, maximum subcutaneous air thickness, and lung re-expansion ratio were all independent predictors of major postoperative complications (Clavien-Dindo grade $\geq$II). Notably, the AUC values for these indices all exceeded 0.7, indicating the significant potential of these objective, readily obtainable imaging markers for early identification of high-risk patients. This capability enables early risk stratification and targeted allocation of medical resources, allowing clinicians to intensify respiratory care, consider proactive interventions, and optimize monitoring for patients identified as high risk before overt clinical deterioration.

The identification of subcutaneous air thickness as a predictor aligns well with pathophysiological logic. Subcutaneous emphysema arises from gas diffusion along tissue planes during surgery, and its severity directly reflects the persistence and extent of abnormal communication between the pleural space/alveoli and the surrounding soft tissues [13]. Significant emphysema is often associated with more extensive tissue dissection and potential persistent micro-leaks, factors which collectively increase the risk of thoracic infection, delayed wound healing, and systemic inflammatory response [14]. Secondly, pneumothorax rate and lung re-expansion ratio, as interrelated indicators, jointly depict the postoperative mechanical environment of the pleural space. A high residual pneumothorax rate combined with a low lung re-expansion ratio indicates failure of the lung to effectively appose the chest wall. This condition not only impairs ventilation and oxygenation but also facilitates pleural fluid accumulation and secondary infection, thereby representing a key mechanism leading to pneumonia and respiratory failure [15,16]. The predictive significance of pleural effusion depth likely lies in its reflection of the intensity of local postoperative inflammatory response, impaired lymphatic drainage, or potential bleeding. A significant pleural effusion can mechanically compress lung tissue, exacerbate atelectasis, and potentially further progress to complicated effusion or empyema [17,18].

Early postoperative CT is already routinely performed in most centers for evaluating complex cases or abnormal symptoms. Our study extends its utility by assigning it a proactive, predictive value. Clinicians can utilize these quantitative indices to identify high-risk patients before the full manifestation of symptoms, thereby facilitating a series of timely, individualized management strategies. Examples include intensified respiratory care for high-risk patients, more active drainage of pleural effusions, consideration of early bronchoscopic suctioning, adjustment of analgesic regimens to facilitate cough and expectoration, and closer monitoring. These approaches align with the principles of enhanced recovery after surgery and precision medicine, shifting the timing of intervention from "reactive management after complication occurrence" to "preventive alert and intervention before complication development".

An interesting finding of our study was that none of the conventional clinical or surgical variables (e.g., age, pulmonary function tests, comorbidities) emerged as independent predictors in the final model, while all four CT indices were highly significant. This pattern may be explained by the relative homogeneity of the carefully selected study cohort, which was limited to clinical stage I

Table 2. Comparison of baseline and CT indices between complication and no-complication groups.

Variables	Total (n = 231)	No Complication (n = 189)	Complication (n = 42)	Statistic	*p*
Age (years), Mean ± SD	62.73 ± 9.80	63.31 ± 9.56	60.10 ± 10.51	$t = 1.94$	0.054
Gender, n (%)				$\chi^2 = 3.48$	0.062
Female	107 (46.32)	93 (49.21)	14 (33.33)		
Male	124 (53.68)	96 (50.79)	28 (66.67)		
BMI (kg/m^2), M (Q_1, Q_3)	23.40 (21.70, 25.75)	23.50 (21.70, 25.80)	23.30 (21.72, 25.27)	Z = –0.26	0.792
FEV_1 (% predicted), Mean ± SD	87.65 ± 13.14	87.84 ± 13.28	86.77 ± 12.62	$t = 0.47$	0.636
DLCO (% predicted), Mean ± SD	85.56 ± 11.63	85.89 ± 11.91	84.05 ± 10.27	$t = 0.93$	0.353
Hypertension				$\chi^2 = 0.17$	0.679
No	142 (61.47)	115 (60.85)	27 (64.29)		
Yes	89 (38.53)	74 (39.15)	15 (35.71)		
Diabetes				$\chi^2 = 3.38$	0.066
No	197 (85.28)	165 (87.30)	32 (76.19)		
Yes	34 (14.72)	24 (12.70)	10 (23.81)		
Coronary artery disease, n (%)				$\chi^2 = 0.00$	1.000
No	204 (88.31)	167 (88.36)	37 (88.10)		
Yes	27 (11.69)	22 (11.64)	5 (11.90)		
COPD, n (%)				$\chi^2 = 0.42$	0.516
No	190 (82.25)	154 (81.48)	36 (85.71)		
Yes	41 (17.75)	35 (18.52)	6 (14.29)		
Smoking, n (%)				$\chi^2 = 1.60$	0.205
No	56 (24.24)	49 (25.93)	7 (16.67)		
Yes	175 (75.76)	140 (74.07)	35 (83.33)		
Pack-years, M (Q_1, Q_3)	32.80 (20.35, 45.55)	32.80 (0.00, 45.20)	37.05 (22.32, 46.30)	Z = –0.87	0.386
Tumor size (cm), M (Q_1, Q_3)	1.80 (1.10, 2.40)	1.80 (1.10, 2.40)	1.90 (1.22, 2.38)	Z = –0.32	0.750
Tumor location, n (%)				$\chi^2 = 1.58$	0.454
Upper lobe	104 (45.02)	87 (46.03)	17 (40.48)		
Middle lobe	26 (11.26)	19 (10.05)	7 (16.67)		
Lower lobe	101 (43.72)	83 (43.92)	18 (42.86)		
Pathological TNM stage, n (%)				$\chi^2 = 0.64$	0.888
IA1	89 (38.53)	74 (39.15)	15 (35.71)		
IA2	97 (41.99)	80 (42.33)	17 (40.48)		
IA3	31 (13.42)	24 (12.70)	7 (16.67)		
IB	14 (6.06)	11 (5.82)	3 (7.14)		
Complex segmentectomy, n (%)				$\chi^2 = 0.38$	0.540
No	163 (70.56)	135 (71.43)	28 (66.67)		
Yes	68 (29.44)	54 (28.57)	14 (33.33)		
Number of segments resected, M (Q_1, Q_3)	1.00 (1.00, 2.00)	1.00 (1.00, 2.00)	1.00 (1.00, 2.00)	Z = –1.76	0.078
Lymph node dissection, n (%)				$\chi^2 = 0.24$	0.626
Systematic	198 (85.71)	163 (86.24)	35 (83.33)		
Lobe-specific	33 (14.29)	26 (13.76)	7 (16.67)		
Operation time (min), M (Q_1, Q_3)	129.00 (109.00, 146.00)	130.00 (109.00, 147.00)	128.50 (109.25, 142.75)	Z = –0.18	0.860
Intraoperative blood loss (mL), M (Q_1, Q_3)	254.00 (147.00, 361.00)	269.00 (162.00, 366.00)	181.50 (126.25, 341.25)	Z = –1.94	0.053
Chest tube duration (days), M (Q_1, Q_3)	5.00 (4.00, 6.00)	5.00 (4.00, 6.00)	8.00 (6.00, 9.00)	Z = –8.19	<0.001
Postoperative hospital stay (days), M (Q_1, Q_3)	6.00 (5.00, 7.00)	6.00 (5.00, 7.00)	9.50 (8.00, 11.00)	Z = –9.89	<0.001
Pleural effusion depth (mm), M (Q_1, Q_3)	11.00 (6.00, 15.50)	10.00 (6.00, 14.00)	20.50 (12.25, 26.75)	Z = –5.74	<0.001
Pneumothorax rate (%), M (Q_1, Q_3)	5.00 (3.00, 9.00)	5.00 (2.00, 7.00)	14.00 (9.00, 17.75)	Z = –6.74	<0.001
Lung re-expansion ratio (%), M (Q_1, Q_3)	87.00 (81.00, 92.00)	89.00 (83.00, 93.00)	78.00 (74.25, 84.00)	Z = –5.77	<0.001
Max subcutaneous air thickness (mm) (%), M (Q_1, Q_3)	7.00 (4.00, 11.00)	6.00 (3.00, 9.00)	14.50 (11.00, 18.00)	Z = –7.11	<0.001

CT, computed tomography; SD, standard deviation; BMI, body mass index; FEV_1, Forced Expiratory Volume in one second; DLCO, Diffusing Capacity of the Lungs for Carbon Monoxide; COPD, Chronic Obstructive Pulmonary Disease; TNM, tumor-node-metastasis.

Table 3. Multivariate analysis.

Variables	β	S.E	Z	p	OR (95% CI)
Pleural effusion depth	0.193	0.047	4.131	<0.001	1.213 (1.107–1.329)
Pneumothorax rate	0.183	0.053	3.430	<0.001	1.201 (1.081–1.333)
Lung re-expansion ratio	–0.137	0.038	–3.585	<0.001	0.872 (0.809–0.940)
Max subcutaneous air thickness	0.363	0.072	5.031	<0.001	1.438 (1.248–1.656)

OR, odds ratio; CI, confidence interval; S.E, standard error.

Table 4. Predictive performance of CT imaging parameters for major complications.

Parameter	AUC (95% CI)	Cutoff	Sensitivity (%)	Specificity (%)	Youden index
Pleural effusion depth (mm)	0.783 (0.720–0.850)	16.5	76.2	71.4	0.476
Pneumothorax rate (%)	0.831 (0.770–0.890)	8.5	78.6	74.6	0.532
Lung re-expansion ratio (%)	0.785 (0.720–0.850)	80.5	73.8	71.4	0.452
Max subcutaneous air thickness (mm)	0.850 (0.790–0.910)	10.5	83.3	78.8	0.621
Combined model	0.961 (0.930–0.990)		88.1	97.4	0.855

AUC, area under the curve.

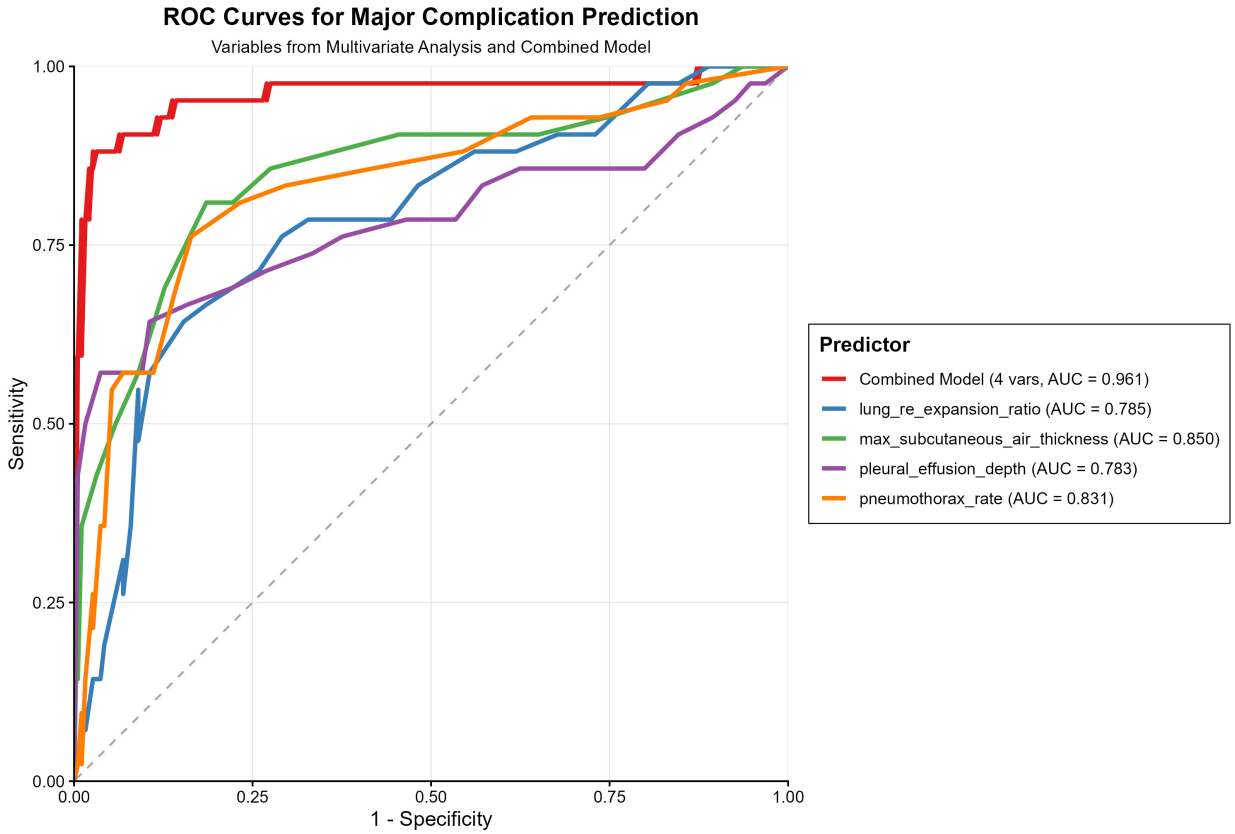

Fig. 1. ROC curves. Note: For ROC analysis, the lung re-expansion rate was converted (100–rate) to align with the risk direction. ROC, receiver operating characteristic; AUC, area under the curve.

patients managed within a standardized enhanced recovery after surgery (ERAS) pathway. This homogeneity likely minimized the variability in traditional risk factors. Nevertheless, it remains possible that in a more heterogeneous cohort with a broader range of comorbidities and functional status, some clinical variables might regain predictive significance. However, this also underscores that, within such a standardized perioperative context, early postoperative imaging findings become the predominant differentiators of complication risk. This observation should be interpreted with caution and not overgeneralized. The absence of clinical predictors does not negate their potential importance in broader, less selected populations. We strongly highlight the need for external validation in more diverse patient populations before our findings can be translated into routine clinical practice.

The combined model that incorporated all four CT parameters achieved an AUC of 0.961, indicating excellent discriminatory power within our cohort. However, such a high AUC value may be partly attributable to overfitting, given the relatively modest sample size and the single-center, retrospective design. Furthermore, the optimism-corrected AUC (0.956) was slightly lower than the apparent AUC, suggesting a degree of model optimism. Therefore, rigorous external validation in independent, preferably multicenter, prospective cohorts is essential to confirm the generalizability of this model and to develop a parsimonious, clinically applicable prediction tool.

This study has several limitations. First, its retrospective, single-center design introduces inherent biases, including selection bias and biases related to institutional practices, which limit the generalizability of the findings. Readers should therefore interpret the high AUC values with caution, as overfitting is a genuine concern. Second, it only assessed CT scans obtained within 2–3 days postoperatively and did not dynamically monitor the trajectory of these indices over time. Third, although important baseline variables were adjusted for, other potential confounding factors (such as precise anesthesia duration, specific segment location, and number of stapler cartridges used) were not fully accounted for. Fourth, the lack of a traditional clinical prediction model for direct comparison limits the ability to quantify the added value of CT indices. Finally, our findings require external validation in independent cohorts before clinical implementation. To mitigate these limitations, prospective multicenter cohorts are required to externally validate our findings before clinical application. Measurements, while performed using specialized software, still required some manual operation. Future research should focus on integrating artificial intelligence approaches, particularly deep learning-based automated segmentation models, to fully automate the extraction of these quantitative indices. Such tools could be integrated into Picture Archiving and Communication Systems (PACS), enabling seamless and real-time risk assessment and clinical alerts at the point of care, thereby facilitating the translation of our findings into routine practice. Based on the findings and limitations of this study, future research could delve into the following directions. Prospective cohort studies are needed to validate the predictive performance of the model established herein and to determine optimal warning thresholds for each index. Investigating the changing patterns of CT indices on serial postoperative scans (e.g., days 1 and 3) may provide superior predictive information. Combining CT quantitative indices with serum inflammatory biomarkers (e.g., Interleukin-6 [IL-6], C-Reactive Protein [CRP]) to jointly construct predictive models from both imaging and molecular perspectives. Developing AI-based fully automated measurement tools and integrating them into PACS to enable real-time risk stratification and automated clinical alerts. Ultimately, randomized controlled trials are required to assess whether intensified interventions based on these CT warning indices can truly reduce complication rates, shorten hospital stays, and improve long-term patient quality of life.

Conclusions

In summary, within the constraints of a retrospective, single-center study, this study confirms that quantitative indices derived from early postoperative CT are robust and objective imaging biomarkers for predicting major complications following thoracoscopic segmentectomy. These indices are readily obtainable in routine clinical practice and may assist surgeons in early identification of high-risk patients. However, prospective, multicenter validation is required before these findings can be translated into routine clinical decision-making.

Availability of Data and Materials

The data that support the findings of this study are available from the corresponding author upon reasonable request.

Author Contributions

WJ designed the research study. WJ, MZ and DZ performed the research. MZ and DZ analyzed the data. WJ drafted the article. All authors contributed to the critical revision of the manuscript for important intellectual content. All authors read and approved the final manuscript. All authors have participated sufficiently in the work and agreed to be accountable for all aspects of the work.

Ethics Approval and Consent to Participate

The study protocol was approved by the Institutional Review Board of The First People's Hospital of Jiashan (2026 Research No. 009). The requirement for informed consent was waived, and the study adhered to the principles of the Declaration of Helsinki.

Acknowledgment

Not applicable.

Funding

This research received no external funding.

Conflict of Interest

The authors declare no conflict of interest.

References

[1] Suzuki K, Watanabe SI, Wakabayashi M, Saji H, Aokage K, Moriya Y, *et al*. A single-arm study of sublobar resection for ground-glass opacity dominant peripheral lung cancer. The Journal of Thoracic and Cardiovascular Surgery. 2022; 163: 289–301.e2. https://doi.org/10.1016/j.jtcvs.2020.09.146.

[2] Saji H, Okada M, Tsuboi M, Nakajima R, Suzuki K, Aokage K, *et al*. Segmentectomy versus lobectomy in small-sized peripheral non-small-cell lung cancer (JCOG0802/WJOG4607L): a

multicentre, open-label, phase 3, randomised, controlled, non-inferiority trial. Lancet. 2022; 399: 1607–1617. https://doi.org/10.1016/S0140-6736(21)02333-3.

[3] Altorki N, Wang X, Kozono D, Watt C, Landrenau R, Wigle D, *et al*. Lobar or Sublobar Resection for Peripheral Stage IA Non-Small-Cell Lung Cancer. The New England Journal of Medicine. 2023; 388: 489–498. https://doi.org/10.1056/NEJMoa2212083.

[4] Bendixen M, Jørgensen OD, Kronborg C, Andersen C, Licht PB. Postoperative pain and quality of life after lobectomy via video-assisted thoracoscopic surgery or anterolateral thoracotomy for early stage lung cancer: a randomised controlled trial. The Lancet. Oncology. 2016; 17: 836–844. https://doi.org/10.1016/S1470-2045(16)00173-X.

[5] Dewapura S, Chu F, Lloyd-Donald P, Francis E, Zhao J, Ratnayake-mudiyanselage P, *et al*. Financial burden of complications in lung resection surgery: scoping review. BJS Open. 2025; 9: zraf057. https://doi.org/10.1093/bjsopen/zraf057.

[6] Zompatori M, Ciccarese F, Fasano L. Overview of current lung imaging in acute respiratory distress syndrome. European Respiratory Review. 2014; 23: 519–530. https://doi.org/10.1183/09059180.00001314.

[7] J Jakobson D, Cohen O, Cherniavsky E, Batumsky M, Fuchs L, Yellin A. Ultrasonography can replace chest X-rays in the post-operative care of thoracic surgical patients. PLoS ONE. 2022; 17: e0276502. https://doi.org/10.1371/journal.pone.0276502.

[8] Bankier AA, Schaefer-Prokop C, De Maertelaer V, Tack D, Jaksch P, Klepetko W, *et al*. Air trapping: comparison of standard-dose and simulated low-dose thin-section CT techniques. Radiology. 2007; 242: 898–906. https://doi.org/10.1148/radiol.2423060196.

[9] Lambin P, Leijenaar RTH, Deist TM, Peerlings J, de Jong EEC, van Timmeren J, *et al*. Radiomics: the bridge between medical imaging and personalized medicine. Nature Reviews. Clinical Oncology. 2017; 14: 749–762. https://doi.org/10.1038/nrclinonc.2017.141.

[10] Gillies RJ, Kinahan PE, Hricak H. Radiomics: Images Are More than Pictures, They Are Data. Radiology. 2016; 278: 563–577. https://doi.org/10.1148/radiol.2015151169.

[11] Kitazawa S, Wijesinghe AI, Maki N, Yanagihara T, Saeki Y, Kobayashi N, *et al*. Predicting Respiratory Complications Following Lobectomy Using Quantitative CT Measures of Emphysema. International Journal of Chronic Obstructive Pulmonary Disease. 2021; 16: 2523–2531. https://doi.org/10.2147/COPD.S321541.

[12] Takahashi Y, Matsuda M, Aoki S, Dejima H, Nakayama T, Matsutani N, *et al*. Qualitative Analysis of Preoperative High-Resolution Computed Tomography: Risk Factors for Pulmonary Complications After Major Lung Resection. The Annals of Thoracic Surgery. 2016; 101: 1068–1074. https://doi.org/10.1016/j.athoracsur.2015.09.009.

[13] Lodhia JV, Tenconi S. Postoperative subcutaneous emphysema: prevention and treatment. Shanghai Chest. 2021; 5.

[14] Ueda K, Hayashi M, Tanaka T, Hamano K. Omitting chest tube drainage after thoracoscopic major lung resection. European Journal of Cardio-Thoracic Surgery. 2013; 44: 225–229. https://doi.org/10.1093/ejcts/ezs679.

[15] Lesser T. Residual Pleural Space after Lung Resection. Zentralblatt Fur Chirurgie. 2019; 144: S31–S42. https://doi.org/10.1055/a-0896-8748.

[16] Rocha E, Jr, de Queiroz FAC, Fonini JS, de Brito JMLT, Mariani AW, Terra RM, *et al*. The use of postoperative X-ray to evaluate residual pleural space and predict infectious pleuropulmonary complications after lung resection for infectious disease. Journal of Thoracic Disease. 2025; 17: 2091–2100. https://doi.org/10.21037/jtd-2024-2022.

[17] Lu C, Jiang F, Pan L, Lin J, Peng Y, Shi H. Risk factor identification and prediction of pleural effusion following coronary artery bypass grafting. American Journal of Translational Research. 2025; 17: 2850–2871. https://doi.org/10.62347/KGKL5899.

[18] Karmy-Jones R, Holevar M, Sullivan RJ, Fleisig A, Jurkovich GJ. Residual hemothorax after chest tube placement correlates with increased risk of empyema following traumatic injury. Canadian Respiratory Journal. 2008; 15: 255–258. https://doi.org/10.1155/2008/918951.